Journal of Hazardous Materials 495 (2025) 138789

Contents lists available at ScienceDirect

Journal of Hazardous Materials

journal homepage: www.elsevier.com/locate/jhazmat

Research Paper

Nearly complete depolymerization of untreated post-consumer plastic with an immobilized and reusable PET hydrolase

Adrián López-Teijeiro [a], Natalia Barreiro-Piñeiro [a], Gemma Eibes [b,*], Jose Martínez-Costas [a,*]

[a] Centre for Research in Biological Chemistry and Molecular Materials (CiQUS), Department of Biochemistry and Molecular Biology, Universidade de Santiago de Compostela, Santiago de Compostela 15782, Spain
[b] CRETUS, Department of Chemical Engineering, Universidade de Santiago de Compostela, Santiago de Compostela 15782, Spain

HIGHLIGHTS

- LCC^{ICCG} hydrolase was self-immobilized in bacteria by a novel one-step methodology.
- The immobilized enzyme exhibits improved thermal and long-term storage stability.
- The immobilized enzyme is reusable for up to 10 cycles with minimal activity loss.
- Untreated post-consumer PET was > 90 % degraded by the immobilized enzyme at 50–70 °C.
- Reused immobilized LCC^{ICCG} fully degraded two post-consumer PET batches in 6 days.

GRAPHICAL ABSTRACT

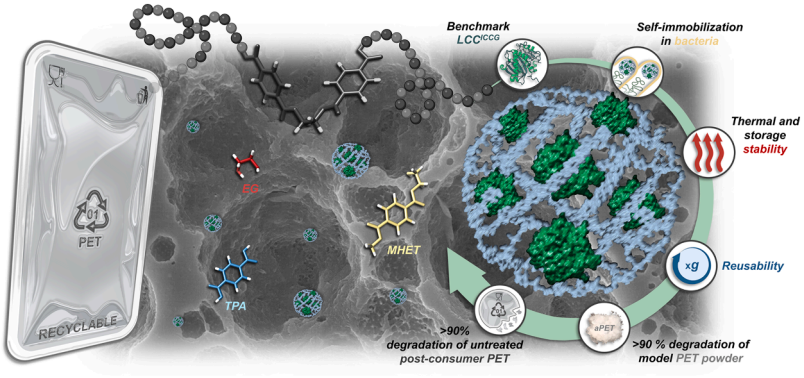

ARTICLE INFO

Keywords:
Polyethylene terephthalate (PET)
Plastic biodegradation
Post-consumer PET
PET hydrolase
LCC^{ICCG}
Enzyme immobilization
Enzyme reutilization

ABSTRACT

The accumulation of plastics in the environment has become a serious concern for the entire society. In recent years, enzyme-based biodegradation has emerged as a promising and sustainable strategy for the recycling of polyethylene terephthalate (PET), one of the most widely used polyester plastics. However, the translation of these technologies to the industrial field faces several underexplored challenges, including the immobilization and reusability of the biocatalysts. Here, we present the use of IC-Tagging as a novel one-step methodology for the "in cellulo" self-immobilization of the benchmark PET-degrading enzyme LCC^{ICCG} in protein nanospheres. The immobilized enzyme showed to be active against soluble substrates and exhibited improved thermal resistance and long-term storage stability, retaining 58 % of relative activity after 3 months at room temperature. Immobilized LCC^{ICCG} also demonstrates remarkable reusability, with minor activity loss up to 10 reuse cycles. Most importantly, nearly complete depolymerization (>90 %) of various untreated amorphous post-consumer PET materials was achieved at a wide range of temperatures (50–70 °C) by removing the products and reusing the enzyme repeatedly. Furthermore, reutilization led to almost full degradation of two consecutive batches of post-consumer PET in 6 days, outperforming all immobilized biocatalysts reported at laboratory scale. Overall,

* Corresponding authors.
E-mail addresses: gemma.eibes@usc.es (G. Eibes), jose.martinez.costas@usc.es (J. Martínez-Costas).

https://doi.org/10.1016/j.jhazmat.2025.138789
Received 10 March 2025; Received in revised form 27 May 2025; Accepted 29 May 2025
Available online 30 May 2025

IC-Tagging emerges as a promising and versatile platform for the production, immobilization and reutilization of top-performing PET hydrolases, contributing to sustainable management of plastic waste.

1. Introduction

Plastics are synthetic polymers that have become a cornerstone of modern human life due to their valuable material properties, including lightweight, durability and economic viability [1,2]. Among these, polyethylene terephthalate (PET) is one of the most widely produced plastics in the world and extensively used in beverage bottles and food packaging [3]. Although different chemical and mechanical methods have been traditionally used for its recycling [4,5], the massive demand for PET and its non-biodegradable nature have led to the accumulation of million tons of plastic waste in landfills and natural environments [6,7]. This ubiquitous presence of plastics raises alarming concerns, as their negative consequences for human health are continuously being reported [8–12]. Therefore, there is an urgent need to develop new sustainable and efficient technologies that contribute to adequate PET end-of-life management.

PET biodegradation based on microorganisms and enzymes has emerged as an environmentally friendly and promising alternative to address plastic recycling [4,13]. Since the depolymerization of PET by hydrolases from the actinomycete *Thermobifida fusca* was first reported 20 years ago [14], numerous research efforts have focused on the use of enzymes for the breakdown of plastics. Importantly, the study of natural bacterial microbial communities conducted to the isolation of leaf-branch compost cutinase (LCC) [15] and PETase from *Ideonella sakaiensis* (*Is*PETase) [16], two PET-degrading enzymes that have been at the forefront of the field in recent years. Many variants of these biocatalysts with improved thermostability and catalytic efficiency have been obtained by advanced protein engineering and computational redesign strategies [13,17]. Remarkably, the quadruple engineered variant of LCC (LCC^{ICCG}) was presented in 2020 and consolidated as the benchmark enzyme for PET biodegradation [18]. LCC^{ICCG} achieved ~90 % depolymerization of pretreated post-consumer PET in 10 h at bioreactor scale [18]. Since then, many promising variants have been designed and proposed as candidates to replace LCC^{ICCG}, such as FastPETase [19], PES-H1$^{L92F/Q94Y}$ [20], HotPETase [21], DepoPETase [22], $ICCG^{I6M}$ [23], $CaPETase^{M9}$ [24], TurboPETase [25] or Kubu-P [26]. However, great interest persists in the discovery of novel enzymes with enhanced efficiency, thermostability, acid tolerance and the ability to degrade semi-crystalline PET [13,27].

Furthermore, the translation of these biocatalysts into a large-scale industrial degradation process requires comprehensive investigation. Different factors including PET pre-treatment, substrate loading or enzyme reusability are critical and have attracted recent attention [13,27]. In this context, immobilization emerges as a powerful strategy to increase operational performance, stability and reusability of PET-degrading enzymes and therefore its industrial prospects [13,27,28]. Although the immobilization of several hydrolases has been extensively reported for synthesis reactions and degradation of soluble substrates [29–33], their use for plastic degradation is limited. Several nanocarriers such as iron oxide nanoparticles, cobalt phosphate nanoflowers, calcium phosphate nanocrystals or mesoporous silica nanoparticles have been used for the immobilization of wild-type PETase or duraPETase variant, either alone or together with MHETase. While these studies have reported significant improvements in the stability, storage and reusability of the biocatalysts, long-term PET depolymerization under mild conditions was required and complete degradation could not be achieved [34–38]. In addition, high loadings of immobilized enzyme were typically employed, limiting the cost-effectiveness of the process. Other strategies including bacterial display or cross-linked enzymes aggregates (CLEAs) have also been explored, but efficient reutilization and high degradation rates remain significant challenges [39,40]. Remarkably, PETase and MHETase have been co-immobilized in CaZn-MOFs, showing great reusability and achieving 90 % weight loss in 5 days at small-scale [41]. More recently, the immobilization of benchmark cutinase variants such as LCC^{FDS}, LCC^{ICCG} or $ICCG_{DAQI}$ have been explored using several strategies including magnetic biochar, hydrogels or stimuli-responsive polymers [42–44]. However, their use has been mainly limited to the degradation of microplastics and nanoplastics, and challenges such as accessibility and reusability hinder further development [44,45].

Hence, the development of new immobilization techniques and their application with highly efficient and benchmark enzymes could represent a valuable tool to support the industrial scale-up of PET biodegradation. In this sense, a novel one-step immobilization system called IC-Tagging has been developed in previous works by our laboratory [46,47]. This methodology is based on the ability of viral-derived protein muNS-Mi to self-assembly and form micro- (MS, in eukaryotic cells) or nanospheres (NS, in bacteria) when it is expressed in a host cell [46–48]. These spheres are able to recruit "in cellulo" any foreign protein labeled with the so-called intercoil tag (IC) when it co-exists in the same cell [46,47]. Thus, the cell itself is able to simultaneously express and immobilize a protein of interest in a carrier, that can be then easily purified by cell lysis and centrifugation in a straightforward and time-efficient manner [46,48]. Since the loaded protein maintains its correct folding, functionality and quaternary interactions in the spheres, complex enzymatic reactions are allowed [49]. Recently, this technology has been used for the immobilization of the industrially relevant enzyme CotA laccase, using bacteria as an efficient expression platform [50]. The loaded enzyme in NS showed high stabilization against pH, elevated temperatures and chemical agents, as well as the ability to be repeatedly reused, unveiling the potential of this methodology to address the challenges in the industrial use of enzymes [50].

Therefore, in the present study we propose the use of IC-Tagging as a novel one-step methodology for the immobilization of PET-degrading enzymes (Fig. 1). To this end, the cutinase LCC^{ICCG} was selected as the gold-standard enzyme for PET depolymerization and immobilized in nanospheres using bacteria as the expression system. The operational conditions and the thermostability of the immobilized enzyme were first evaluated using soluble substrates and compared with the free enzyme. Furthermore, its potential applicability for PET degradation was validated using model substrates as well as different post-consumer materials. In addition, the possibility of repeatedly reusing the immobilized enzyme was thoroughly investigated.

2. Methods

2.1. Bacterial strains and chemicals

Escherichia coli (*E. coli*) XL1-Blue (Agilent Technologies) was used for plasmid amplification. *E. coli* BL21 CodonPlus RP (DE3) (Agilent Technologies) and *E. coli* Rosetta-gami B(DE3) (Merck) were used for protein expression. All chemical reagents used were of analytical grade and were obtained at the highest purity from Sigma-Aldrich if not stated otherwise.

2.2. Plasmids construction

All enzyme sequences used were codon-optimized for *E. coli* expression. The coding sequence of LCC^{ICCG} (mutant $LCC^{F243I/D238C/S283C/Y127G}$; GenBank ID for LCC: AEV21261) [18] was synthesized and cloned into a pUC plasmid by Integrated DNA technologies.

For immobilization of LCC^{ICCG}, two tagged versions were obtained,

with the IC-tag either at the N-terminus (IC-LCC^{ICCG}) or C-terminus (LCC^{ICCG}-IC). In addition, the SV5 epitope sequence (5′-GGCAAACCAATCCCAAACCCACTGCTGGGCCTGGAT-3′) was included in the constructions to facilitate enzyme detection by Western blot. On the one hand, to express IC-LCC^{ICCG}, the sequence of LCC^{ICCG} was obtained by PCR amplification from the plasmid pUC LCC^{ICCG} with the forward primer 5′-GGGGTACCTCTAACCCGTACCAGCGT-3′ and the reverse primer 5′- CCGCTCGAGTTATTCCAGCTGGCAGTG-3′ and cloned into plasmid pcDNA 3.1/Zeo containing the IC-tag sequence followed by the SV5 sequence to obtain plasmid pcDNA 3.1/Zeo IC-SV5-LCC^{ICCG}. Then, the whole construct IC-SV5-LCC^{ICCG} was amplified using the forward primer 5′-GGAGATCTCGCGGAAGATCACTTGTTGGC-3′ and reverse primer 5′-CCGCTCGAGTTATTCCAGCTGGCAGTG-3′ and cloned into the second polylinker of the plasmid pETDuet-1 muNS-Mi [48] to generate the pETDuet-1 muNS-Mi/IC-SV5-LCC^{ICCG}. On the other hand, to express LCC^{ICCG}-IC, the sequence of LCC^{ICCG} was obtained by PCR amplification from the plasmid pUC LCC^{ICCG} with the forward primer 5′-CGGGATCCCTCTAACCCGTACCAGCGT-3′ and the reverse primer 5′-GCTCTAGATTCCAGCTGGCAGTGACGGTTG-3′ and cloned into plasmid pcDNA 3.1/Zeo containing the SV5 sequence followed by the IC-tag sequence to obtain plasmid pcDNA 3.1/Zeo LCC^{ICCG}-SV5-IC. Then, the whole construct LCC^{ICCG}-SV5-IC was amplified using the forward primer 5′-CGGGATCCCTCTAACCCGTACCAGCGT-3′ and reverse primer 5′-CCGCTCGAGCGGTTACGCTTCCACACG-3′ and cloned into the second polylinker of the plasmid pETDuet-1 muNS-Mi to generate the pETDuet-1 muNS-Mi/LCC^{ICCG}-SV5-IC.

For the expression of free LCC^{ICCG}, the construct LCC^{ICCG}-SV5 was obtained by PCR amplification from the plasmid pcDNA 3.1/Zeo LCC^{ICCG}-SV5-IC with the forward primer 5′-CATGCCATGGCCTCTAACCCGTACCAGCG-3′ and the reverse primer 5′-CCGCTCGAGATCCAGGCCCAGCAGTGGG-3′, and cloned in the plasmid pET-21d(+) (containing an C-terminal 6xHis-tag) to generate pET-21d(+) LCC^{ICCG}-SV5.

2.3. Expression and purification of free LCC^{ICCG}

For the expression of free LCC^{ICCG}, *E. coli* BL21-CodonPlus-RP (DE3) was transformed with pET-21d(+) LCC^{ICCG}-SV5. A single colony of transformed bacteria was inoculated into Luria Bertani (LB) medium with 100 μg mL^{-1} ampicillin and grown overnight at 37 °C and 200 rpm. This preculture was diluted 25-fold in LB and grown until the optical density at 600 nm (OD_{600}) reached 0.4–0.6. Expression was then induced by adding 1 mM isopropyl-1-thio-β-D-galactopyranoside (IPTG) and culture was incubated overnight at 18 °C and 200 rpm. After induction, cells were harvested by centrifugation (7000×*g*, 4 °C, 10 min) and the pellet was washed twice with phosphate-buffered saline (PBS; 100 mM KPi pH 8.0, 300 mM NaCl) and frozen. For the purification, the bacterial pellet was thawed and resuspended in lysis buffer (50 mM Tris-HCl pH 7.5, 300 mM NaCl, 20 mM imidazole). Then, lysozyme (1 mg mL^{-1}) was added, and cells were incubated at 37 °C during 30 min. After that, bacteria were disrupted by sonication (6 cycles of 30-seconds pulse on/30 seconds pulse off) and debris was removed by centrifugation (7000×*g*, 4 °C, 30 min). The soluble fraction was incubated with Ni Sepharose 6 Fast Flow resin (Cytiva) for 1 h and unbound proteins were washed with 3 volumes of lysis buffer. Bound LCC^{ICCG} was eluted with elution buffer (50 mM Tris-HCl pH 7.5, 300 mM NaCl, 250 mM imidazole) and dialyzed against the storage buffer (20 mM Tris-HCl pH 8, 300 mM NaCl) to remove imidazole. Purified enzyme concentration was determined using the DC Protein Assay Kit (Bio-Rad), following the manufacturer's instructions. The purity of the purified protein was evaluated by sodium dodecyl sulfate-polyacrylamide gel electrophoresis (SDS-PAGE). The identity of the enzyme was confirmed by Western-blot analysis using a mouse monoclonal antibody against SV5 Tag (ThermoFisher) and a secondary peroxidase-conjugated anti-mouse antibody (Sigma-Aldrich).

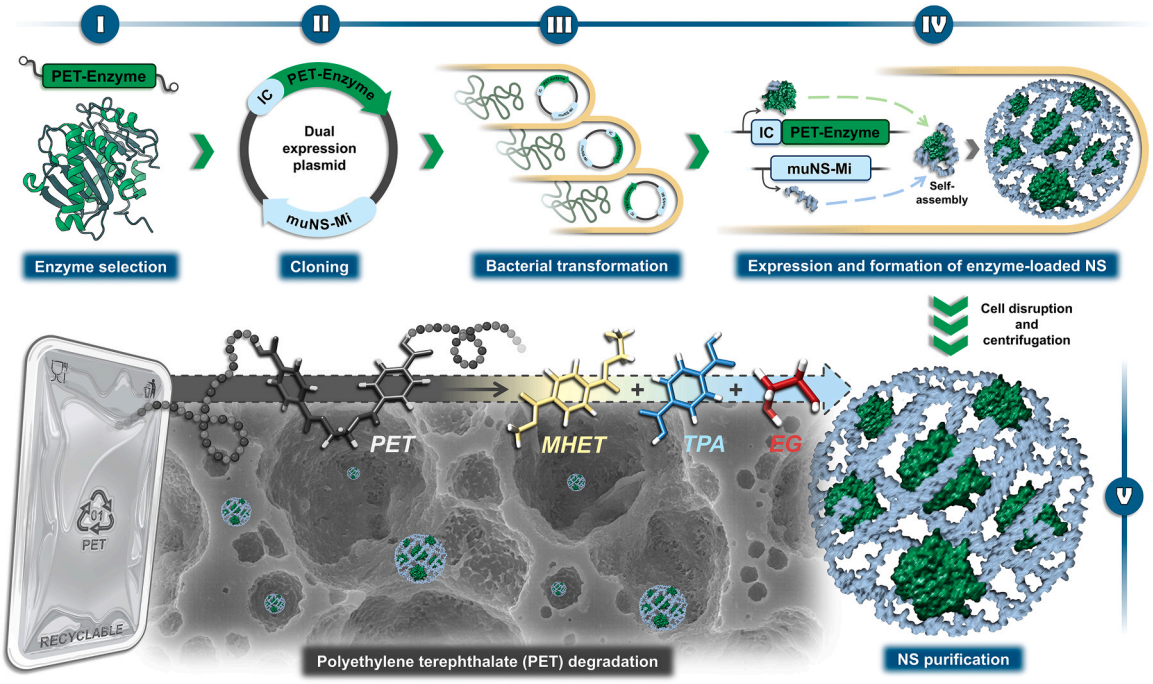

Fig. 1. IC-Tagging methodology as a platform for the one-step immobilization of PET-degrading enzymes. Once the PET-degrading enzyme of interest has been selected (I), its sequence is labeled with the IC-tag at either N- or C-terminus and cloned into a dual plasmid for co-expression with the scaffold protein muNS-Mi (II). The plasmid is then used to transform bacteria (III) followed by the induction of expression and subsequent self-immobilization "in cellulo" (IV). After that, the immobilized enzyme in nanospheres (NS) is purified by cell lysis and centrifugation (V) and can be directly used for the degradation of PET materials into intermediate products (mostly MHET, but also BHET) and its constituent monomers (TPA and EG). A simplified scheme of PET depolymerization is represented.

2.4. Expression and purification of immobilized LCC^{ICCG}

For the expression of immobilized LCC^{ICCG}, *E. coli* BL21-CodonPlus-RP (DE3) or *E. coli* Rosetta-gami B(DE3) was transformed with the corresponding plasmid (pETDuet-1 muNS-Mi/IC-SV5-LCC^{ICCG} or pETDuet-1 muNS-Mi/LCC^{ICCG}-SV5-IC). A single colony of transformed bacteria was inoculated into LB medium with 100 μg mL^{-1} ampicillin and grown overnight at 37 °C and 200 rpm. This preculture was diluted 25-fold in LB and grown until the OD_{600} reached 0.4–0.6. Expression was then induced by adding IPTG at the concentration indicated in each experiment (0.1 or 1 mM), and culture was incubated at temperatures and times also indicated (18 or 37 °C; 3 h or overnight). After induction, cells were harvested by centrifugation (7000×*g*, 4 °C, 10 min) and the pellet was washed twice with PBS and frozen. For the purification, the bacterial pellet was thawed and resuspended in lysis buffer (0.25 % Tween-20, 1 mM DTT, 200 mM NaCl, 20 mM Tris pH 7.5, 2 mM $MgCl_2$). Then, lysozyme (1 mg mL^{-1}) was added, and cells were incubated at 37 °C during 30 min. After that, bacteria were disrupted by three passes through a French Press and NS were recovered by centrifugation (2700×*g*, 4 °C, 5 min). The NS were then washed 3 times in RB+ buffer (10 mM HEPES pH 7.9; 10 mM KCl; 5 mM $MgCl_2$) containing 0.5 % Triton X-100 and 3 other times in RB+ buffer. Finally, the NS was transferred to RB- storage buffer (10 mM HEPES pH 7.9, 10 mM KCl, 0.5 mM EDTA). The presence of each NS protein component (enzyme and muNS-Mi) was evaluated by SDS-PAGE and their concentration was determined by densitometric analysis comparing serial dilutions of NS with serial dilutions of bovine serum albumin (BSA, Sigma-Aldrich) of known concentrations, using Quantity One 1-D Analysis Software (Bio-Rad). The identity of immobilized LCC^{ICCG} was confirmed by Western-Blot analysis as explained above for the free enzyme. The identity of muNS-Mi was confirmed using a rabbit polyclonal antibody against avian reovirus S1133 muNS protein (raised in our laboratory) and a secondary peroxidase-conjugated anti-rabbit antibody (Sigma-Aldrich).

2.5. TEM and SEM analysis of immobilized LCC^{ICCG}

For transmission electron microscopy (TEM) analysis of cells containing NS, induced bacteria were centrifuged (2700×*g*, 4 °C, 5 min), washed 3 times in PBS and fixed with 2 % glutaraldehyde in PBS for 20 min. Then, bacteria were washed 6 times with Milli-Q water and ultra-thin sections of the final pellet were obtained with a Leica Ultracut UCT ultramicrotome. The sections were washed to grids and stained with 2 % uranyl acetate/Reynolds lead citrate and observed in a TEM JEOL JEM-1011.

For scanning electron microscopy (SEM) analysis of purified NS, the nanospheres were fixed with 4 % formaldehyde in PBS for 15 min with gentle shaking. Fixed NS were dialyzed against RB- buffer and the final samples were deposited on silicon wafer substrate and dried for 48 h at 37 °C prior to analysis by ZEISS FESEM Ultra Plus.

2.6. DLS and ELS analysis of immobilized LCC^{ICCG}

The size distribution and polydispersity index (PdI) of the purified NS were determined by dynamic light scattering (DLS), and the Z-potential was measured by electrophoretic light scattering (ELS). In both cases, the NS were diluted in RB- buffer to a concentration of 10 μg_{NS} mL^{-1}. DLS and ELS were analyzed using a ZEN0040 cuvette and a DTS1070 capillary cell, respectively, in a Zetasizer NANO ZSP instrument (Malvern Instruments). All measurements were performed in triplicate.

2.7. Activity and kinetics assays of LCC^{ICCG} using soluble substrates

Standard activity assay for LCC^{ICCG} was performed using *p*-nitrophenyl acetate (*p*NPA) according to a previously reported method [15, 34]. Briefly, 0.25 μg mL^{-1} of the enzyme was incubated with 1 mM *p*NPA (dissolved in ethanol) in 50 mM Tris-HCl pH 7.5 buffer (total volume of 1 mL). The activity of the enzyme was continuously monitored observing the release of *p*-nitrophenol by measuring the absorbance at 405 nm ($\varepsilon_{405\ nm}$=18,600 M^{-1}cm^{-1}) for 3 min at 25 °C. A blank reaction without enzyme was performed in all cases to subtract the effect of *p*NPA autohydrolysis. One unit (U) of activity was defined as the amount of enzyme necessary to hydrolyze 1 μmol of *p*NPA per min. Measurements were performed using a Jasco V-770 UV/Vis-Visible/NIR Spectrophotometer. All reactions were conducted in triplicate.

To determine reaction kinetics, activity was measured under standard conditions with *p*NPA concentrations ranging from 0.0675 to 8 mM. The initial rate was calculated and plotted against *p*NPA concentrations. Parameters were determined from Michaelis-Menten model by nonlinear least-squares regression analysis using GraphPad Prism (v8.0.1). The experiment was conducted in triplicate.

The activity of LCC^{ICCG} was also tested using BHET as a substrate. In this case, 0.25 μg mL^{-1} of the enzyme was incubated with 1 mM BHET (dissolved in water) in 50 mM Tris-HCl pH 7.5 buffer (total volume of 1 mL) for 30 min at 60 °C. Reaction was stopped by diluting with one volume of 50 mM citrate-phosphate pH 4 and heating at 100 °C for 10 min and hydrolysis of BHET was analyzed by high-performance liquid chromatography (HPLC). A control reaction without enzyme was included in the experiment, but negligible products were detected. One unit (U) of activity was defined as the amount of enzyme necessary to hydrolyze 1 μmol of BHET per min. Reactions were performed in triplicate.

2.8. Effect of pH and temperature in LCC^{ICCG} activity

To study the optimal pH and temperature of free and immobilized LCC^{ICCG}, activity towards *p*NPA was assayed under standard conditions modifying the buffer (50 mM citrate-phosphate buffer pH 5–7 or 50 mM Tris-HCl pH 7.5–10) or the temperature (20–90 °C). The activity at optimum pH and temperature for each enzyme was considered as 100 %, and relative activities were calculated accordingly. In addition, thermal resistance of the enzymes was studied by incubating them in 50 mM Tris-HCl pH 7.5 at selected temperatures (50–70 °C). Samples were withdrawn at 3, 6, 24 and 48 h of incubation and residual activity towards *p*NPA was assayed under standard conditions. The initial activity was set as 100 %, and residual activities were calculated accordingly over time. All reactions were performed in triplicate.

2.9. Reusability and storage of immobilized LCC^{ICCG}

To study the reusability of immobilized LCC^{ICCG}, 10 consecutive cycles of *p*NPA hydrolysis under standard conditions were conducted. After each cycle, enzyme was recovered by centrifugation (20,000×*g*, 4 °C, 10 min), washed once in RB- buffer, and used for the next cycle with fresh substrate solution. The activity in the first cycle was established as 100 % and relative activities in the following cycles were calculated accordingly. Reutilization was also followed by SDS-PAGE analysis of enzyme after each cycle. The experiment was performed in triplicate.

To study the storage stability of free and immobilized LCC^{ICCG}, enzymes were incubated in 50 mM Tris-HCl pH 7.5 at room temperature (24 ± 2 °C). Samples were withdrawn at 2 weeks, 1, 2 and 3 months of incubation and residual activity towards *p*NPA was assayed under standard conditions. The initial activity was set as 100 %, and residual activities were calculated accordingly over time.

2.10. Degradation assays using aPET

Amorphous PET (aPET) beads were kindly provided by Novapet company (crystallinity of ~3.8 %, dimensions of 0.2 ×0.1 ×0.1 cm and approximately 15 mg). Before degradation, beads were washed with 20 % ethanol and distilled water, and dried overnight at 37 °C. Preliminary assays were performed to study the effect of pH, buffers,

temperature, agitation and solvents in degradation. Generally, aPET bead was soaked in 50 mM HEPES pH 9.0 (total volume of 1 mL) with 1 mg_{enzyme} g_{PET}^{-1} for 24 h at 70 °C and 1000 rpm in a ThermoMixer C (Eppendorf) modifying buffer and pH (potassium-phosphate pH 7.0–8.0, sodium-phosphate pH 7.0–8.0, Tris-HCl pH 7.0–9.0, HEPES pH 7.0–9.0 and Glycine-NaOH pH 9.0–10.0 at a concentration of 50 mM in all cases), temperature (40–70 °C) or agitation (0–1500 rpm). The effect of solvents and detergents (ethylene glycol, DMSO, glycerol, ethanol and SDS) was studied by adding them in the reaction media at the concentrations indicated in each experiment.

For long-term reactions, aPET bead was soaked in 50 mM HEPES pH 9.0 (1 mL of reaction) with 1 mg_{enzyme} g_{PET}^{-1} for 72 h and 1000 rpm at 70, 60 and 50 °C. For reused immobilized LCC^{ICCG} with buffer exchange, the NS were recovered every 24 h by centrifugation (20,000×*g*, 10 min), the supernatant with the released products removed, and the enzyme resuspended in fresh reaction buffer. Weight loss of aPET beads as a result of degradation was determined gravimetrically and their surface was observed by SEM alongside the reaction.

For complete depolymerization assays, aPET beads were micronized for 1 min using a CGoldenwall HC-150 Grinder mill in the presence of dry ice. After sieving, the fraction between 200 and 500 μm was recovered, washed with 20 % ethanol and distilled water, dried overnight at 37 °C, and used for degradation experiments. Thus, 15 mg of aPET powder was soaked in 50 mM HEPES pH 9.0 (total volume of 1 mL) with 1 mg_{enzyme} g_{PET}^{-1} at 1000 rpm and 70, 60 and 50 °C during the time needed to achieve the maximum possible degradation, resulting in 72, 96 or 192 h, respectively. For reused immobilized LCC^{ICCG} with buffer exchange, the enzyme was recovered, and buffer renewed every 24 h as above, with the exception of the reaction at 50 °C, when the buffer exchange was performed at 24, 48, 72, 96 and 168 h.

For all reactions, samples were withdrawn over time to estimate the total released products by UV absorbance. In addition, for long-term reactions with aPET beads and powder, PET monomers released were analyzed by HPLC at the end of the reaction. Estimated degradation (%) of aPET powder at the end of the reaction was calculated from mM TPA+MHET quantified by HPLC. A control reaction without enzyme was included in all experiments, but negligible products were detected. All experiments were performed in triplicate.

2.11. Degradation assays using post-consumer PET

Post-consumer PET materials were obtained from a fruit package (PcPET-1, crystallinity of 6.9 %), nuts package (PcPET-2, crystallinity of 5 %) and multiwell package (PcPET-3, crystallinity of 2.3 %) and cut into small squares (0.5 ×0.5 cm, approximately 10 mg). Before degradation, materials were washed with 20 % ethanol and distilled water, and dried overnight at 37 °C. Thus, 10 mg of each Pc-PET was soaked in 50 mM HEPES pH 9.0 (total volume of 1 mL) with 1 mg_{enzyme} g_{PET}^{-1} at 1000 rpm and 70, 60 and 50 °C during the time needed to achieve the maximum possible degradation, resulting in 72, 96 h or 14 days, respectively. For reused immobilized LCC^{ICCG} with buffer exchange, the enzyme was recovered, and buffer renewed every 24 h as above, except for the reaction at 50 °C, when the reutilization was performed at 24, 48, 72, 96, 168, 216 and 264 h. At the end of the reaction, PET monomers released were analyzed by HPLC.

For degradation at larger-scale with the immobilized enzyme, ~250 mg of PcPET-3 was soaked in 50 mM HEPES pH 9.0 (12 mL of reaction) with 1 mg_{enzyme} g_{PET}^{-1} for 72 h at 70 °C and 1000 rpm. The immobilized enzyme was recovered and buffer renewed at 9, 24, 33, 48 and 57 h as above.

For the complete degradation of two successive batches with the immobilized enzyme, 10 mg of PcPET-3 was soaked in 50 mM HEPES pH 9.0 (total volume of 1 mL) with 1 mg_{enzyme} g_{PET}^{-1} at 70 °C and 1000 rpm. The immobilized enzyme was recovered and buffer exchanged every 24 h as above. When non-residual PET was observed, the enzyme was recovered and another 10 mg of PcPET-3 were added to start a new cycle. Again, NS were successively recovered and buffer renewed every 24 h until nearly complete depolymerization of second batch was achieved.

For all reactions, samples were withdrawn over time to estimate the total released products by UV absorbance. The weight loss of PcPET materials as a result of degradation was determined gravimetrically. A control reaction without enzyme was included in all experiments, but negligible products were detected. All experiments were performed in triplicate.

2.12. Estimation of soluble products by UV absorbance

The time-course of PET degradation was monitored by UV absorbance. Since BHET, MHET and TPA share an absorbance peak at 240–244 nm, absorbance can be used to estimate the overall sum of released products [27,52–55]. Commercial MHET (BLD Pharmatech) was selected as the reference as it showed more similar results to those obtained by HPLC, and its standard curve at 240 nm was generated using a Jasco V-770 UV/Vis-Visible/NIR Spectrophotometer. Samples were withdrawn at different times during PET degradation and absorbance at 240 nm was measured. If necessary, samples were diluted in the reaction buffer. Absorbance value was used to estimate the sum of soluble PET hydrolysis products according to the Lambert-Beer law and expressed as mM $MHET_{eq}$. Absorbance measurements of each replicate (n = 3) were performed in duplicate.

2.13. Quantification of soluble products by HPLC

At the end of the reactions, the PET monomers released (BHET, MHET and TPA) were analyzed by HPLC. Samples were accordingly diluted in distilled water and 100 μL were injected in the column. The analyses were performed in a Jasco XLC HPLC (Jasco Co.) equipped with a 3110 MD diode array detector (detection at 240 nm) and a GEMINI C18 column (3 μm, 150 ×4.6 mm) maintained at 30 °C (Phenomenex). The mobile phase consisted of a solution of acetonitrile (A) and distilled water containing 0.1 % (v/v) formic acid (B) at a flow rate of 0.8 mL min^{-1}. A gradient elution was programmed from 5 % B solution to 100 % B in 14 min, hold for 3 min and return to 5 % B in 2 min. Amounts of hydrolysis products were calculated using standard curves prepared for commercial TPA (Sigma-Aldrich), BHET (Sigma-Aldrich) and MHET (BLD Pharmatech). As the amounts of BHET were negligible in all the reactions, they were not considered for the analyses.

2.14. DSC of PET materials

The crystallinity of PET materials was estimated using differential scanning calorimetry (DSC) instrument (Q200, TA instrument). For each material, 10 mg of sample were equilibrated at 30 °C and heated to 300 °C at a heating rate of 20 °C min^{-1}. Heat of fusion (ΔHm) and cold crystallization (ΔHc) were calculated by integrating the areas under the peaks using TA Universal Analysis software. The enthalpy of melting for a fully crystalline PET material (ΔHf) is 140.1 J g^{-1}. Thus, the percent of crystallinity was calculated with the following equation:

$$\%Crystallinity(Xc) = \frac{\Delta Hm - \Delta Hc}{\Delta Hf} \times 100 \quad (1)$$

2.15. SEM analysis of aPET beads

The surface of aPET beads during degradation was observed by SEM. aPET beads were recovered at indicated times, washed with 20 % ethanol and distilled water and then dried overnight at 37 °C. Then, each bead was mounted on sample stubs and a sputter gold-coating was applied to make them conductive. The samples were analyzed using a FESEM Zeiss Ultra Plus.

2.16. Data analysis and statistics

Data analysis was performed using GraphPad Prism (v8.0.1) software. Data are generally presented as mean ± standard deviation (s.d.); the number of replicates is indicated in each figure. An unpaired two-tailed t-test (α=0.05) was performed to evaluate the existence of significative differences between the free and immobilized LCC^{ICCG}.

3. Results

3.1. Optimization of the expression, purification, and characterization of immobilized LCC^{ICCG}

Since LCC^{ICCG} has been established as the benchmark enzyme for PET degradation, the development of complementary technologies to improve its feasibility and viability for large-scale industrial applications would be of significant interest [13,28]. Among these, enzyme immobilization emerges as a promising underexplored strategy that can be assessed using the IC-Tagging platform. Therefore, for its loading and immobilization in nanospheres, the coding sequence of LCC^{ICCG} was initially fused with the IC-tag. To anticipate any possible negative effects on enzyme folding, two versions were obtained, bearing the IC-tag either at the N-terminus (IC-LCC^{ICCG}) or at the C-terminus (LCC^{ICCG}-IC). Both constructs were cloned into the second polylinker of a dual plasmid containing the muNS-Mi sequence [51], to enable their co-expression and promote enzyme loading into the NS (Fig. 2a). To optimize the immobilization procedure, several bacterial strains and expression conditions were evaluated. In particular, BL21 CodonPlus RP(DE3) and Rosetta-gami B(DE3) strains were transformed with each IC-tagged construct, and expression was performed under different temperatures (18 or 37 °C), incubation times (3 h or overnight) and inducer concentrations (0.1 or 1 mM of IPTG). A total of 14 immobilized versions were obtained and successfully purified following a previously described protocol [48] (Supplementary Fig. 1a). To compare the catalytic performance of the different versions, a soluble and small substrate (*p*NPA, *p*-nitrophenyl acetate) was selected for the spectrophotometric determination of the esterase activity as previously described [34,52]. The best results were observed for BL21 expressions at 37 °C for both LCC^{ICCG}-IC and IC-LCC^{ICCG}, demonstrating that the enzyme performance does not depend on IC-tag location (Fig. 2b). Interestingly, the optimal temperature for the expression of NS LCC^{ICCG} contrasted with the free enzyme, whose expression has been extensively reported at low temperatures [18,25–27] and has also been expressed and purified accordingly in this study (Supplementary Fig. 2a,b). For the 4 most active versions of immobilized LCC^{ICCG}, higher purification yields as well as an appropriate ratio of enzyme/muNS-Mi (close to 1:1) were considered as selection criteria (Supplementary Fig. 1b), alongside the effect of temperature in the activity due to its importance in PET

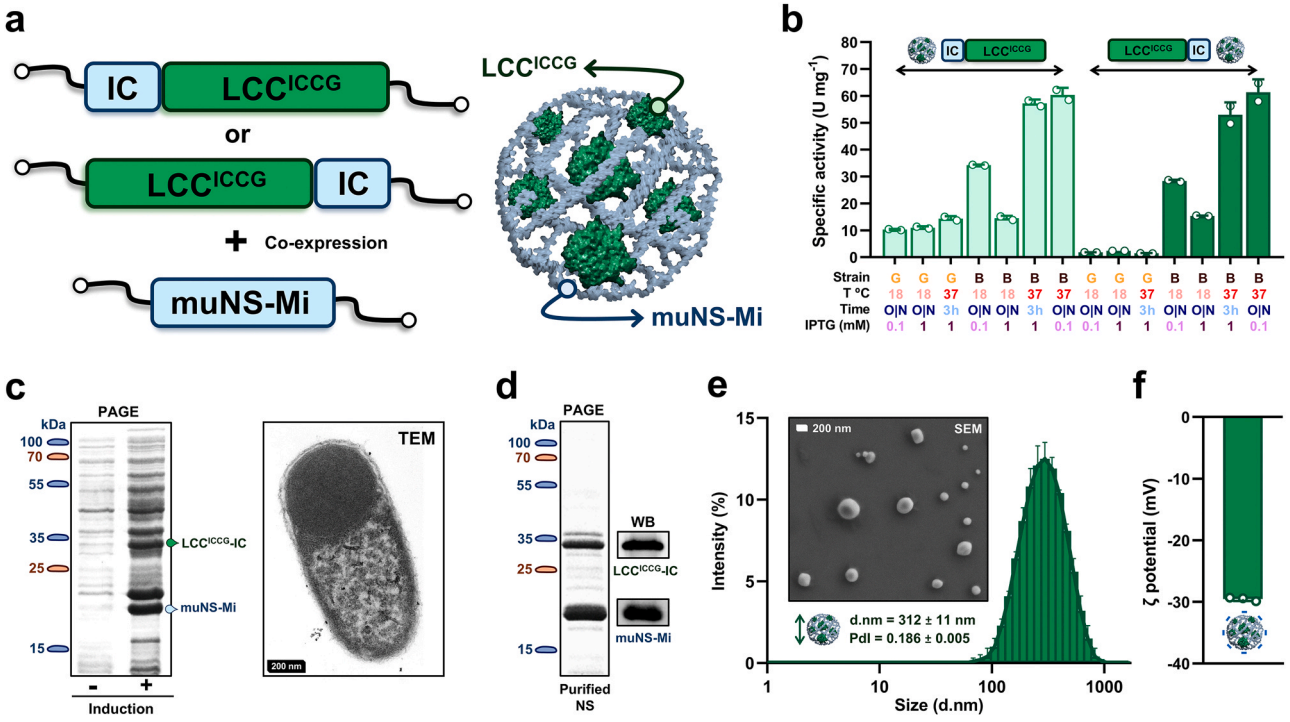

Fig. 2. Expression, purification and structural characterization of immobilized LCC^{ICCG}. a. Schematic illustration of IC-tagged LCC^{ICCG} constructions and formation of enzyme-containing nanospheres. Two versions were obtained, with the tag either at the N-terminus (above) or at the C-terminus (below). The co-expression of the constructs with muNS-Mi sequence in bacteria leads to the immobilization of the enzyme in protein nanospheres (right). b. Specific activity (*p*NPA as a model substrate) for different expression versions of immobilized LCC^{ICCG}. A total of 7 conditions were tested for the expression of each construct by modifying bacterial strain (Rosetta-Gami B(DE3), G; BL21 CodonPlus RP(DE3), B), temperature (18 or 37 °C), incubation time (3 h or overnight, O|N) and inducer concentration (0.1 or 1 mM). Reactions were performed in duplicate (n = 2) under standard conditions (50 mM Tris-HCl pH 7.5 at 25 °C and 1 mM *p*NPA) using purified NS; data are presented as mean values ± standard deviation (s.d.) and individual values are shown (circles). Considering these results together with purification yields, enzyme/muNS-Mi ratio and the temperature profiles (see Supplementary Fig. 1), immobilized LCC^{ICCG}-IC expressed O|N in BL21 strain at 37 °C and induced with 0.1 mM IPTG, hereafter referred as NS LCC^{ICCG}, was selected for the following experiments. c. Expression and formation of NS LCC^{ICCG} in bacteria. Co-expression of LCC^{ICCG} and muNS-Mi was checked by SDS-PAGE analysis of total bacterial extracts (left). Extracts from non-induced (-) and IPTG-induced (+) bacteria are shown. The correct formation of nanospheres inside the bacteria was confirmed by TEM (right, a representative bacterium with a nanosphere is shown). d. SDS-PAGE and Western Blot analysis of purified NS LCC^{ICCG}. Bands corresponding to enzyme and muNS-Mi are shown. e. Structural characterization of purified NS LCC^{ICCG}. DLS intensity-based size distribution histogram and SEM image of NS are shown. The average size of NS (d.nm) and polydispersity index (PdI) are indicated. f. ζ potential of NS LCC^{ICCG}. DLS and ζ potential measurements were performed in triplicate (n = 3); data are presented as mean values ± s.d. and individual values are shown for ζ potential data (circles).

degradation [13,27] (Supplementary Fig. 1c). Thus, immobilized LCC^{ICCG}-IC expressed overnight in BL21 strain at 37 °C and induced with 0.1 mM IPTG, hereafter referred as NS LCC^{ICCG}, was selected for the rest of the experiments and further characterized.

First, the proper formation of the NS LCC^{ICCG} inside the bacteria was checked by transmission electronic microscopy (TEM), in concordance with the correct co-expression of LCC^{ICCG}-IC and muNS-Mi evidenced by SDS-PAGE analysis of total cell extracts after induction (Fig. 2c). Then, NS LCC^{ICCG} purification was also verified by SDS-PAGE, showing the simultaneous co-purification of the two proteins involved, whose identity was further confirmed by Western Blot analysis (Fig. 2d). Notably, determination of purification yields for the immobilized enzyme showed a ~30 % increase compared to the free enzyme under our conditions (Supplementary Fig. 2c). Finally, the preservation of NS integrity after the purification procedure was proven by scanning electron microscopy (SEM) and dynamic light scattering (DLS), showing a monodisperse distribution of around 300 nm (Fig. 2e). Also, the surface charge of NS was established as strongly negative (Fig. 2f). In summary, correctly formed nanospheres loaded with active LCC^{ICCG} were successfully produced in bacteria and purified for functional characterization.

3.2. Determination of catalytic performance and stability of immobilized LCC^{ICCG}

To evaluate the impact of immobilization on the catalytic performance of LCC^{ICCG}, the enzymatic activity and the influence of operational conditions (pH and temperature) were characterized and compared to the free enzyme using *p*NPA as a model soluble substrate (Fig. 3a). Under standard conditions (50 mM Tris-HCl pH 7.5 at 25 °C and 1 mM of substrate), the immobilized enzyme showed to be active against *p*NPA, with a 22 % reduction in the specific activity compared to free LCC^{ICCG} (Fig. 3b). Comparable results (28 % reduction) were obtained when bis(2-hydroxyethyl) terephthalate (BHET), a soluble intermediate of PET degradation, was tested as a substrate (Supplementary Fig. 3a). A deeper analysis of catalytic parameters against *p*NPA revealed that the immobilized enzyme appears to exhibit a 2.1-fold increase in the substrate affinity (2.1 lower K_M) at the expense of a 2.3-fold reduction in maximum velocity (V_{max}) (Supplementary Fig. 3b and Supplementary Table 1). These differences result into a closer overall kinetic efficiency (k_{cat}/K_M) in both cases (Supplementary Table 1).

In addition, the effect of pH and temperature on esterase activity against *p*NPA was investigated. On the one hand, both free and NS LCC^{ICCG} showed an optimum pH of 8, whereas the immobilized version exhibits an extended operational pH range, maintaining higher activity at lower values (6.0–7.5) (Fig. 3c). On the other hand, immobilization also slightly expanded the operational temperature range, since higher relative activities were observed at lower temperatures compared to the free enzyme (Fig. 3d). Beyond the optimum temperature, thermal resistance of enzymes is critical considering that effective PET

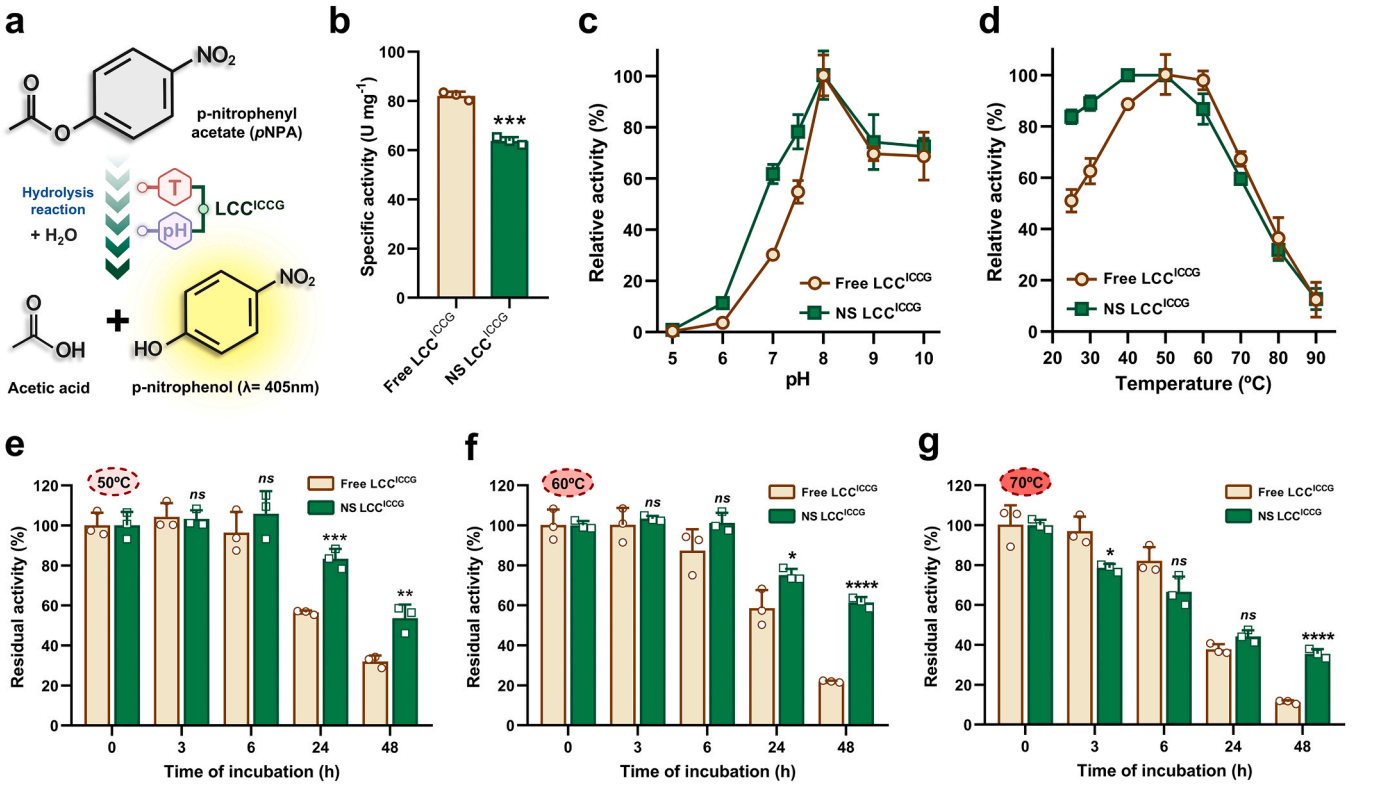

Fig. 3. Catalytic performance and thermal stability of free and immobilized LCC^{ICCG}. a. Schematic representation of esterase assay based on *p*-nitrophenyl acetate (*p*NPA). LCC^{ICCG} catalyze substrate hydrolysis to *p*-nitrophenol (*p*NP), which can be spectrophotometrically quantified at 405 nm. pNPA was used to study the effect of pH and temperature in the catalytic performance of free and immobilized LCC^{ICCG}. b. Comparative specific activity of free (brown bars) and immobilized LCC^{ICCG} (green bars) towards *p*NPA under standard conditions (50 mM Tris-HCl pH 7.5 at 25 °C and 1 mM *p*NPA). c. Effect of pH in the activity of free (brown bars) and immobilized LCC^{ICCG} (green bars). The activity at optimum pH was set as 100 %, and relative activities were calculated accordingly. d. Effect of temperature in the activity of free (brown bars) and immobilized LCC^{ICCG} (green bars). The activity at optimum temperature was considered as 100 %, and relative activities were calculated accordingly. e-g. Thermal stability of free (brown bars) and immobilized LCC^{ICCG} (green bars) after the incubation at 50 (e), 60 (f) and 70 °C (g) for 48 h. The initial activity was set as 100 %, and residual activities were calculated accordingly over time. In all cases, experiments were performed in triplicate (n = 3); data are presented as mean values ± s.d. and individual values are shown in graphs b,e-g (circles and squares for the free and immobilized enzyme, respectively). Statistical analyses using an unpaired two-tailed *t*-test (ns: not significant, $p > 0.05$, *$p < 0.05$, **$p < 0.01$, ***$p < 0.001$, ****$p < 0.0001$) were performed to compare the activity of the free and immobilized enzyme.

hydrolysis must be performed at elevated temperatures [13,27]. Therefore, the stability at 50, 60 and 70 °C was evaluated. In general, immobilized LCC^{ICCG} showed similar behavior to the free enzyme during the first hours of incubation but maintained significative higher residual activity after long times. Particularly, an increase of 1.7-fold, 2.8-fold and 3.1-fold in residual activity was observed for the immobilized enzyme after 48 h of incubation at 50, 60 and 70 °C, respectively (Fig. 3e–g). Overall, the results obtained indicate that immobilized LCC^{ICCG} is active against small and soluble substrates with a reduction in the specific activity compared to the free version, which is countered by a slight extension of the operational pH and temperature ranges as well as an increase in thermal resistance specifically at long incubation times.

3.3. Reutilization and storage stability of immobilized LCC^{ICCG}

Considering the expected large-scale use of LCC^{ICCG} for PET degradation, the possibility of reusing the enzyme during several cycles as well as its long-term storage under mild conditions would be of enormous interest. Since loaded nanospheres obtained by IC-Tagging methodology can be easily recovered from the reaction media through centrifugation or microfiltration, reusability of the enzyme can be implemented [50]. This could be integrated in a PET degradation process, enabling not only successive cycles of complete depolymerization but also the progressive removal of degradation products during a single batch (Fig. 4a). Therefore, the reusability of immobilized LCC^{ICCG} was initially tested using *p*NPA as a substrate. It was found that the enzyme can be reused for up to 10 consecutive cycles maintaining almost 70 % of the initial activity (Fig. 4b). The reduction in activity may be mostly due to the inevitable residual loss of nanospheres during the recovery process (Supplementary Fig. 4a-c). The addition of divalent ions (Mg^{+2} or Ca^{+2}) to promote nanosphere aggregation or the implementation of more efficient recovery systems (such as microfiltration membranes) could contribute to reduce this potential loss. Additionally, the storage stability of the immobilized enzyme was studied by measuring the residual activity towards *p*NPA during 3 months of incubation at room temperature (24 ± 2 °C) and compared to the free enzyme. Despite the considerable stability of the free enzyme during the first month of incubation, NS LCC^{ICCG} retained 2.3-fold residual activity (58 vs 25 %) after 3 months of storage (Fig. 4c). Together, these results demonstrate that reusability and long-term storage of immobilized LCC^{ICCG} is feasible, contributing to its potential industrial application.

3.4. Functional validation of immobilized LCC^{ICCG} for degradation of model PET substrates

To assess the ability of immobilized LCC^{ICCG} for the degradation of plastic, amorphous PET (aPET) beads were used for preliminary experiments (Fig. 5a and Supplementary Fig. 5a). Initially, optimal degradation conditions of the immobilized enzyme were investigated and compared with the free enzyme. Particularly, the effect of pH, temperature and agitation was studied in a 24-h reaction and total released products were estimated by UV absorption at 240 nm from a MHET standard curve, similar to previously described [27,52–55] (Supplementary Fig. 6). On the one hand, 70 °C and 50 mM HEPES pH 9.0 buffer were selected as optimal conditions for efficient PET degradation for both free and NS LCC^{ICCG} (Supplementary Fig. 7b,c). On the other hand, the increase in velocity of agitation was translated into a relevant higher degradation yield for both versions (Supplementary

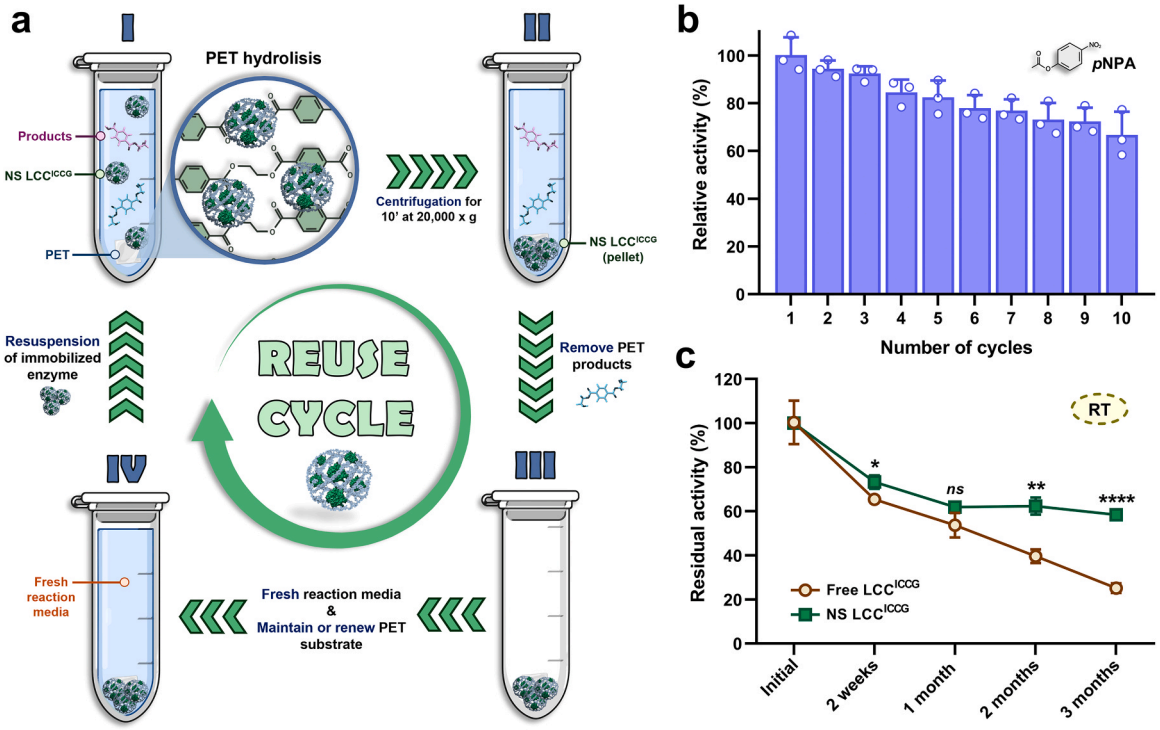

Fig. 4. Reusability and storage stability of immobilized LCC^{ICCG}. a. Schematic illustration of a PET degradation process based on the reutilization of immobilized LCC^{ICCG}. At the end or during degradation (I), the enzyme can be easily recovered by centrifugation (II). After that, the released products are removed as well as fresh reaction buffer is added, maintaining or renewing the PET substrate (III and IV). Finally, the immobilized enzyme is resuspended, and a new cycle is initiated (I). b. Reusability of immobilized LCC^{ICCG} using *p*NPA as a substrate. The activity in the first cycle was established as 100 % and relative activities in the following cycles were calculated accordingly. Experiment was performed in triplicate (n = 3); data are presented as mean values ± s.d. and individual values are shown (circles). c. Storage stability of free and immobilized LCC^{ICCG} at room temperature (24 ± 2 °C). The initial activity against *p*NPA was set as 100 %, and residual activities were calculated accordingly over time. Experiment were performed in triplicate (n = 3); data are presented as mean values ± s.d. Statistical analyses using an unpaired two-tailed *t*-test (ns: not significant, $p > 0.05$, *$p < 0.05$, **$p < 0.01$, ***$p < 0.001$, ****$p < 0.0001$) were performed to compare the residual activity of the free and immobilized enzyme over time.

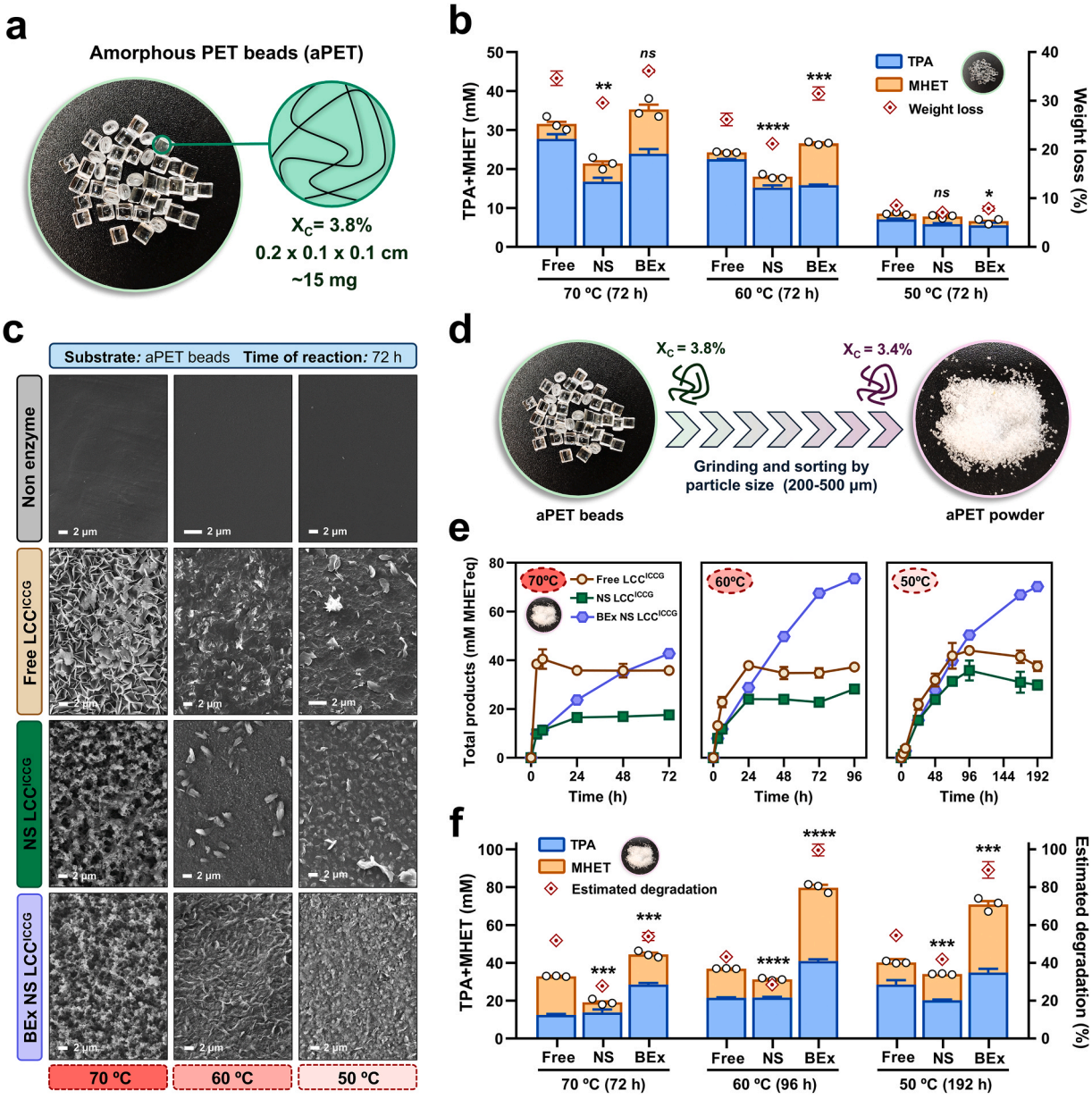

Fig. 5. Degradation of aPET beads and powder by the free and immobilized LCC^{ICCG}. a. Crystallinity (X_C) and physical characteristics of aPET beads. Dimensions (length x width x height) and weight (mg) of a single bead is indicated. b. Comparison of PET hydrolytic activity of free, immobilized (NS) and reused immobilized LCC^{ICCG} with buffer exchange (BEx) towards aPET beads at 70, 60 and 50 °C for 72 h. Total monomers released (sum of MHET and TPA quantified by HPLC) are represented with blue/orange (TPA/MHET) bars (left y-axis), and weight loss (%) is indicated with red diamonds (right y-axis). c. SEM images of the surface of aPET beads degraded by the free, immobilized (NS) and reused immobilized LCC^{ICCG} with buffer exchange (BEx) after 72 h at 70, 60 and 50 °C. aPET beads subjected to incubation without enzyme were used as negative control. d. Schematic representation of aPET powder generation from aPET beads. Crystallinity (X_C) of obtained material is indicated. e. Time course of PET hydrolytic activity of free (brown circles), immobilized (green squares) and reused immobilized LCC^{ICCG} (blue hexagons) towards aPET powder at 70, 60 and 50 °C for 72, 96 or 192 h, respectively. For reused NS LCC^{ICCG}, enzyme was recovered and buffer renewed at the times at which total products were measured. The total released products were estimated over time by UV-absorbance based on a MHET standard (MHETeq). f. Comparison of PET hydrolytic activity of free, immobilized LCC^{ICCG} (NS) and reused immobilized LCC^{ICCG} with buffer exchange (BEx) towards aPET powder at 70, 60 and 50 °C for 72, 96 or 192 h, respectively. Total monomers released (sum of MHET and TPA quantified by HPLC) are represented with blue/orange (TPA/MHET) bars (left y-axis), and estimated degradation (%) is indicated with red diamonds (right y-axis). All PET degradation reactions were performed at pH 9.0 using 15 mg_{aPET} mL^{-1} (total volume of 1 mL) and 1 mg_{enzyme} g_{aPET}^{-1}. All experiments were performed in triplicate (n = 3); data are presented as mean values ± s.d., and individual values are shown in graphs b,c (white circles). Statistical analyses using an unpaired two-tailed *t*-test (ns: not significant, $p > 0.05$, *$p < 0.05$, **$p < 0.01$, ***$p < 0.001$, ****$p < 0.0001$) were performed to compare the PET monomers released by the free and immobilized enzyme.

Fig. 7d) and was therefore implemented for the rest of the experiments. Then, the influence of IC-Tag location on PET degradation was evaluated. Although the LCC^{ICCG}-IC version was selected based on *p*NPA assays (Fig. 2b and Supplementary Fig. 1), the position of the IC-Tag at either N- or C-terminus could potentially affect enzyme exposure in the nanospheres, which is expected to be critical when acting on a solid substrate such as PET. Interestingly, no relevant differences in the amount of released products were observed between the LCC^{ICCG}-IC and IC-LCC^{ICCG} versions (Supplementary Fig. 8), suggesting that IC-tag location does not substantially impact the accessibility of the immobilize enzyme to PET. Finally, the effect of different organic solvents (ethylene glycol, DMSO, glycerol and ethanol) and detergents (SDS) on

PET degradation was studied. As these compounds are used for plastic cleaning prior to recycling (e.g. SDS or ethanol), enzyme tolerance to their residual persistence is required for practical applications [33]. Furthermore, the use of some of these solvents (e.g. DMSO or ethylene glycol) has been reported to have positive effects on plastic depolymerization [56–58]. In our case, their presence at low concentrations (10 % for ethylene glycol, DMSO and glycerol; 1 % for ethanol; 0.01 % for SDS) in the reaction media does not seem to positively or negatively impact the PET degradation efficiency, with similar effect for both free and immobilized LCC^{ICCG} (Supplementary Fig. 9).

Once conditions were established, a 72-h reaction was performed using aPET beads in the range of 50–70 °C. The release of soluble products was monitored over time by UV absorbance and the amount of MHET and TPA was quantified by HPLC at the end of the reaction. To exploit the reusability of the immobilized enzyme, degradation was also performed by repeated 24-h cycles of recovering and reusing the enzyme together with exchange of the reaction buffer (Fig. 4a), and compared to the batch reaction by the free or NS LCC^{ICCG}. As expected, the degradation rate was generally improved at higher temperatures, and the free enzyme showed a better performance than the immobilized enzyme in a batch reaction (Fig. 5b, Supplementary Fig. 10 and Supplementary Table 2). However, differences were considerably smaller as the temperature was reduced, with no significant differences at 50 °C in the total released products (Fig. 5b and Supplementary Table 2). Thus, the recover and reuse of the immobilized enzyme together with the removal of products allowed to improve the degradation efficiency when a fastest reaction was conducted (60 and 70 °C), reaching equal or even higher final degradation yields compared to the free enzyme (Fig. 5b and Supplementary Table 2). While the batch reactions gradually slowed down after 24 h, the possibility of exchange the buffer and reuse the enzyme allowed to maintain an almost linear degradation rate over time (Supplementary Fig. 10). This may be due to inhibition by accumulated products and pH reduction rather than thermal deactivation of the enzyme, since the addition of new enzyme each 24 h did not increase degradation yield (Supplementary Fig. 11). This would also explain why the effect of buffer exchange is not relevant when a low amount of products have been generated, as observed in the reaction at 50 °C (Fig. 5b and Supplementary Fig. 10). In addition, degradation of aPET was analyzed by SEM along the reactions (Fig. 5c and Supplementary Fig. 12). Degradation was evident in all cases, as well as the existence of greater surface erosion at 70 °C after 72 h, consistently with the expected thermal increase of PET crystallinity and priority in attacking amorphous regions [59] (Fig. 5c and Supplementary Fig. 12). Moreover, significant differences in the surface roughness of aPET beads degraded by the free and immobilized at 70 °C were observed, consistent with the differences in the total amount of released products (Fig. 5b and Supplementary Fig. 13). Interestingly, morphological differences in surface erosion were observed in the PET beads among the free and immobilized enzyme (Fig. 5c and Supplementary Fig. 12), which could be indicating unknown differences in the accessibility or degradation pattern for both versions.

In any case, the maximum depolymerization achieved was ~35 % of weight loss with any of the versions, most probably due to the thickness and inaccessibility of the material used (Fig. 5a). Since having an enzymatic system that allows complete depolymerization is essential to consider the efficient industrial application of the process [13,27], aPET beads were grinded and 200–500 μm powder fraction was used as a new amorphous model substrate with higher surface area (Fig. 5d and Supplementary Fig. 5b). Beyond that the degradation yields were significantly higher than aPET beads at all temperatures, free enzyme maintained a better general degradation ratio compared to the immobilized LCC^{ICCG} in a batch reaction, with smaller differences at lower temperatures (Fig. 5e and Supplementary Table 3). Remarkably, buffer exchange and reutilization of the enzyme led to almost complete depolymerization (>90 %) of aPET powder at 60 and 50 °C in 96 and 192 h, respectively (Fig. 5f and Supplementary Table 3). Particularly, 79.7 mM and 70.9 mM of total products were released at 60 and 50 °C, respectively, which represents a 2.2-fold and 1.8-fold that of free enzyme in a batch reaction (Fig. 5f and Supplementary Table 3). Even at 70 °C, reutilization almost tripled the degradation of non-reused immobilized enzyme and conduced to a 25 % increase compared to the free enzyme (Fig. 5f and Supplementary Table 3).

In short, the immobilized enzyme proved to be able to degrade aPET in both bead and powder form. While the degradation efficiency is generally slightly reduced compared to the free enzyme in a batch reaction, particularly at elevated temperatures, the possibility of easily recovering and reusing the enzyme together with buffer exchange significantly enhances the overall performance, even leading to almost full depolymerization at low temperatures when enough surface area of reaction is available.

3.5. Evaluation of immobilized LCC^{ICCG} in the degradation of untreated post-consumer PET materials

To test the real applicability of immobilized LCC^{ICCG}, different post-consumer PET (PcPET) materials widely used for packaging of common products and with different crystallinity, molecular weight or thickness were collected and their degradation was assessed. In particular, amorphous samples with crystallinities in the range of 2–7 % were obtained from fruit and nuts packages (PcPET-1 and PcPET-2, respectively) and from containers of laboratory consumables (PcPET-3) (Fig. 6a and Supplementary Fig. 5c-e). All untreated materials were directly degraded in the range of 50–70 °C with the free and immobilized enzyme (with buffer exchange or not) during the time needed to achieve the maximum depolymerization rate. As it has been observed for model PET materials, degradation yield was dependent on temperature and the free enzyme showed a higher rate than the immobilized enzyme at 70 °C in a batch reaction (Supplementary Fig. 14a), although differences were non-significant in the sum of released products at the end of the reaction for most materials (Fig. 6b). However, the performance of NS LCC^{ICCG} equaled the free enzyme at 60 °C (Fig. 6c and Supplementary Fig. 14b) and was considerably higher at 50 °C in a batch reaction (Fig. 6d and Supplementary Fig. 14c), as NS LCC^{ICCG} released > 25 % of total products than free enzyme after 14 days of reaction for all materials (Fig. 6d and Supplementary Table 4). Interestingly, NS LCC^{ICCG} showed a higher TPA yield than the free enzyme at the end of all reactions, which was not observed with the model materials (Fig. 6b-d and Supplementary Table 4). Most importantly, enzyme reutilization and buffer exchange enabled nearly complete depolymerization (>90 % of weight loss) of almost all PcPET materials at 70, 60 and 50 °C within 72 h, 96 h and 14 days, respectively, with the exception of PcPET-1 at 70 °C (~60 % of weight loss) as well as PcPET-1 and PcPET-3 at 50°C (~80 % of weight loss) (Fig. 6b-e, Supplementary Fig. 14a-c and Supplementary Table 4). This contrasts with the maximum weight loss of 50–60 % achieved by the free or immobilized enzyme in a batch reaction (Fig. 6b-e and Supplementary Table 4). The marked increase in crystallinity observed at 70°C for PcPET-1 (from 6.9 % to >20 % after 48 h of degradation), mainly attributed to thermal physical aging, could explain the inability to achieve complete degradation, even with buffer exchange (Supplementary Fig.5 and Supplementary Fig. 15). In contrast, the crystallinity increase was more moderate for the other materials (from 5 % to ~15 % for PcPET-2 and from 2.3 % to ~11 % for PcPET-3), allowing nearly complete depolymerization and demonstrating the capability of the immobilized enzyme to degrade semicrystalline PET (Supplementary Fig. 15). In addition, these results were faithfully replicated when higher PET loading was used. Specifically, ~250 mg of PcPET-3 were almost completely degraded (~98 % of weight loss) in 72 h at 70 °C when the buffer was periodically exchanged and enzyme reused (Supplementary Fig. 16). Finally, the possibility of using the immobilized enzyme for the depolymerization of more than one batch of untreated post-consumer PET was studied. To this end, PcPET-3 was degraded at 70 °C by repeatedly exchanging the buffer and reusing the

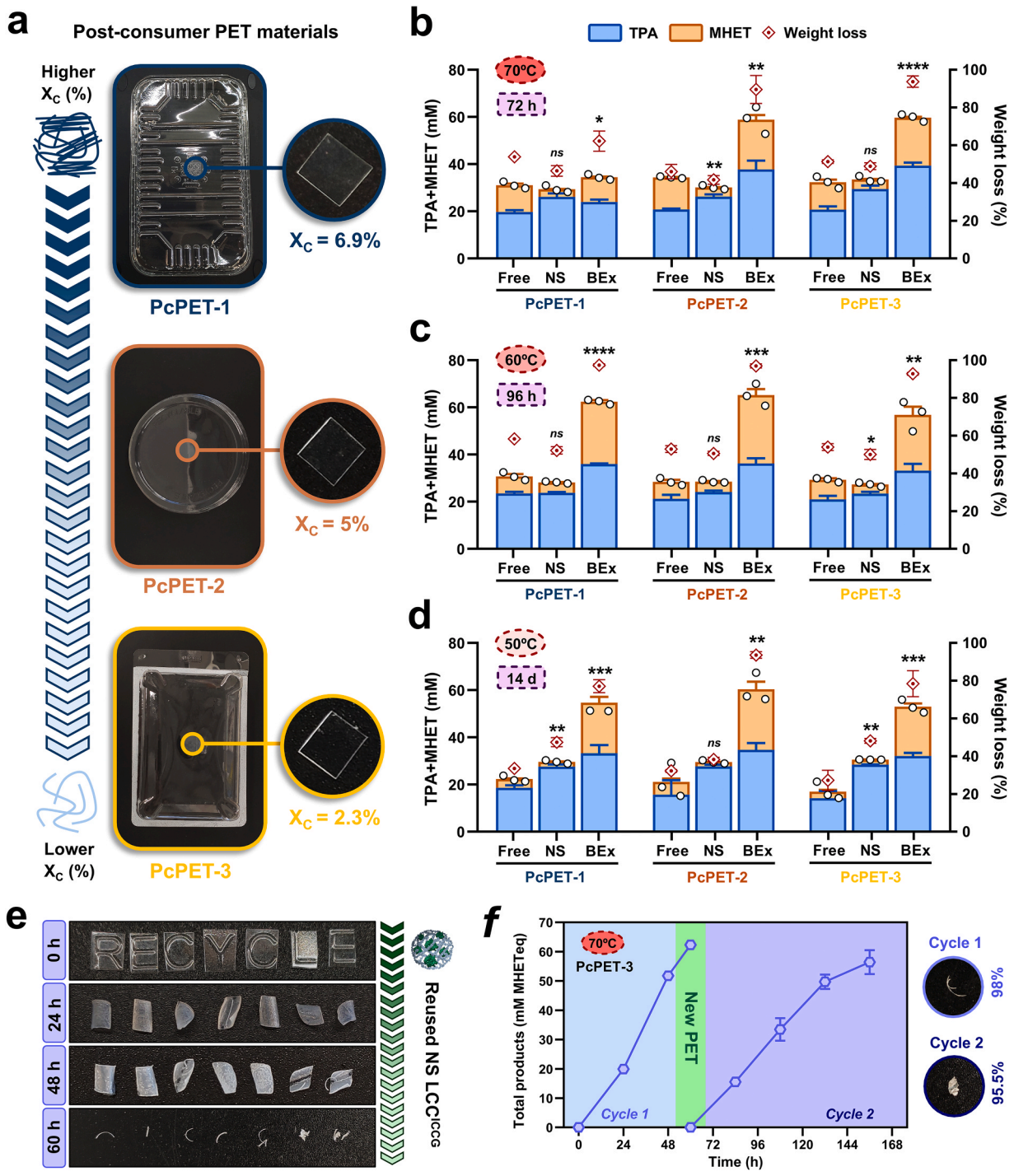

Fig. 6. Degradation of untreated post-consumer PET by the free and immobilized LCC^{ICCG}. a. Post-consumer PET materials used for degradation. Crystallinity (X_C) for each material is indicated. b-d. Comparison of PET hydrolytic activity of free, immobilized LCC^{ICCG} (NS) and reused immobilized LCC^{ICCG} with buffer exchange (BEx) towards different PcPET materials at 70 (b), 60 (c) and 50 °C (d) for 72 h, 96 h or 14 days respectively. Total monomers released (sum of MHET and TPA quantified by HPLC) are represented with blue/orange (TPA/MHET) bars (left y-axis) and weight loss (%) is indicated with red diamonds (right y-axis). Statistical analyses using an unpaired two-tailed *t*-test (ns: not significant, $p > 0.05$, *$p < 0.05$, **$p < 0.01$, ***$p < 0.001$, ****$p < 0.0001$) were performed to compare the PET monomers released by the free and immobilized enzyme. e. Complete degradation of PcPET-3 by reused immobilized LCC^{ICCG} with buffer exchange at 70 °C. f. Complete degradation of two batches of PcPET-3 by reused immobilized LCC^{ICCG} at 70 °C. The immobilized enzyme was recovered and buffer renewed at the times at which total products were measured. After nearly complete depolymerization of the first batch, enzyme was recovered and used to start a second batch with a new loading of PET. The total released products were estimated over time by UV-absorbance based on a MHET standard (MHETeq). Weight loss (%) reached in each cycle is indicated. All PET degradation reactions were performed at pH 9.0 using 10 mg_{PcPET} mL^{-1} (total volume of 1 mL) and 1 mg_{enzyme} g^{-1}_{PcPET} All experiments were performed in triplicate (n = 3); data are presented as mean values ± s.d., and individual values are shown in graphs b-d (white circles).

enzyme. Once the first batch was nearly fully depolymerized, a second batch with a new load of PcPET-3 was started. Although the degradation rate of the second batch was slightly lower due to the inevitable residual loss of enzyme activity, the almost complete degradation of the two batches was achieved in 60 and 96 h, respectively (Fig. 6f).

In short, the immobilized enzyme is able to efficiently degrade untreated amorphous post-consumer PET, with minor differences or even being superior compared to the free enzyme in a batch reaction. Furthermore, the progressive reuse of the enzyme together with buffer exchange allowed to achieve almost full depolymerization of all materials studied and at a wide range of temperatures, as well as to completely degrade two consecutive batches of PcPET.

4. Discussion

The enormous advances recently made in enzyme-based PET biodegradation have been accompanied by the need for its large-scale industrial deployment [27,28]. Among other strategies, immobilization methods are promising to obtain robust and reusable biocatalysts and contribute to industrial operational requirements [13,27,28,60]. Here, we report a novel one-step self-immobilization strategy for the reusability of PET hydrolases, selecting LCC^{ICCG} as a widely recognized benchmark enzyme [18]. The characterization of the immobilized enzyme using soluble substrates revealed a slight decrease in the specific activity compared to the free enzyme. Steric hindrance of the catalytic active site by the scaffold protein could explain the reduced activity [44], while substrate binding did not seem to be altered as shown by the kinetic analysis. Other effects such as potential slight distortion of the LCC^{ICCG} structure or conformational changes due to the presence of the muNS-Mi scaffold, and limited substrate accessibility to enzyme molecules located in the inner regions of the nanospheres, should also be considered as possible drawbacks. However, the extension of optimal pH range, increased thermostability, reusability and long-term storage were provided by the immobilization. Interestingly, the positive effect of immobilization on the thermostability of LCC^{ICCG} appears to be lower than in our previous studies with other industrial enzymes, such as CotA laccase [50]. The intrinsic stability of LCC^{ICCG} combined with its highly optimized structure, may have reduced the potential benefits of our system.

Substrate accessibility and deficient mass transfer are important bottlenecks that have limited the development of immobilization technologies for the degradation of macromolecular substrates such as PET [28,44,45]. As our methodology generates interspersed systems in which the immobilized enzyme is indistinctly located inside and on the surface of the nanospheres, we hypothesized that degradation of a solid substrate would be feasible. Indeed, immobilized LCC^{ICCG} was able to degrade model PET materials and untreated post-consumer plastic over a wide range of temperatures at a slightly slower rate than the free enzyme, probably due to intrinsic reduced activity or accessibility issues. Importantly, these differences were higher at 70 °C but insignificant at lower temperatures, possibly related to the extension of the operational temperature range observed for the immobilized enzyme. Also, accessibility deficiencies may be more relevant near the glass transition temperature of PET (>70 °C), since thermal-induced crystallization is accompanied by a reduction in the available amorphous degradable regions [27,56]. In addition, the degradation mechanism of the enzyme loaded in the nanospheres remains unclear. While the immobilized enzyme on the surface could mainly act on the solid substrate, biocatalyst molecules present in the inner part could be exclusively dedicated to the degradation of intermediate released products, complementing and improving the depolymerization. This could explain the higher TPA/MHET ratio observed in some reactions using the immobilized enzyme, as enzyme molecules located in the inner regions of the nanospheres may primarily contribute to the hydrolysis of BHET and MHET. However, further studies are needed to deeply understand the functioning of the immobilized enzyme.

As product accumulation during PET degradation leads to a decrease in the pH of the reaction buffer [27], batch reactions under standard substrate loadings used in this study were limited to ~50 % depolymerization. However, the possibility of recovering and reusing the enzyme allowed the periodic removal of products and avoided enzyme inhibition, reaching nearly complete degradation of PET powder as well as post-consumer materials and suggesting that enzymatic rates should be improved at reactor scale with controlled pH. Moreover, this strategy confirmed the high thermostability of the immobilized enzyme as well as the non-affectation of the recovery process, since linear degradation was maintained for 72 h, 96 h and 14 days at 70, 60 and 50 °C, respectively.

To date, a limited number of studies have focused on the immobilization of PET-degrading enzymes and complete depolymerization was rarely achieved [34–40] (Supplementary Table 5). Here, our immobilized LCC^{ICCG} proved to almost completely degrade post-consumer PET in less than 72 h at 70 °C, but also at lower temperatures in long-term reactions, outperforming all immobilized biocatalysts reported at laboratory scale and demonstrating great reusability. In particular, a maximum of 20 $g_{PcPET}\ L^{-1}$ was degraded with 1 $mg_{enzyme}\ g^{-1}_{PcPET}$. In two consecutive cycles of nearly complete degradation of pcPET, a depolymerization yield of ~0.30 $g_{PcPET}\ mg^{-1}_{enzyme}\ d^{-1}$ was achieved, which represents a ~14 % increase compared to the performance of the immobilized biocatalyst reported by Zhang et al. [41] (~0.26 $g_{PET}\ mg^{-1}_{enzyme}\ d^{-1}$ in 2 cycles). Both studies greatly improve all the other immobilized PET enzymes at small-scale, where complete depolymerization is not achieved and only one cycle is performed (Supplementary Table 5). More recently, Fritzsche et al. [44] used a pH-responsive polymer for $ICCG_{DAQI}$ immobilization, reaching nearly complete degradation of PET fibers at reactor scale in 14 h, although low substrate loading (10 $g_{PET}\ L^{-1}$) and high catalyst concentration (3 $mg_{enzyme}\ g^{-1}_{PET}$) were required. However, the disparity of degradation conditions and the lack of appropriate data from the other immobilization studies make reliable comparisons difficult, so standardized experiments are needed.

In addition, the use of IC-Tagging system presents several significant advantages over other reported methods for the immobilization of PET-degrading enzymes. Most existing approaches are based on the covalent attachment or directed binding of free enzymes to different inorganic nanocarriers or polymeric scaffolds (e.g. iron oxide nanoparticles, mesoporous silica nanoparticles, cobalt phosphate nanoflowers, CaZn-MOFs or hydrogels) [34–38,40,42–45], or on the cross-linking of purified proteins using chemical agents (CLEAs) [40,44] (Supplementary Table 5). These methods require the separate expression and purification of the recombinant enzyme and the preparation of the nanocarriers with the appropriate modifications to enable their efficient coupling. Moreover, traditional systems rarely achieve an immobilization yield of 100 %, limiting the overall efficiency of the process [36,41,44]. In contrast, our technology offers a one-step self-immobilization procedure in which the bacterium itself is able to simultaneously express and immobilize the enzyme, reducing both the complexity and cost of the process. Furthermore, purification of the immobilized enzyme is simpler and less time-consuming than for free enzymes, as no sophisticated chromatography systems are required and nanospheres can be easily recovered by centrifugation. Importantly, the immobilized system described here is entirely protein-based and thus inherently biodegradable, minimizing environmental persistence and long-term accumulation are expected to be minimal. Conversely, conventional methods involve the use of inorganic materials, cross-linking agents and stabilizing chemicals, which may present environmental risks and warrant careful evaluation. These features suggest that the scalability of the IC-Tagging system could overcome several challenges that have hindered the application of other immobilization methods at large-scale, such as the low stability of functionalized supports, the reliance on expensive and hazardous reagents or batch-to-batch reproducibility issues [60]. Despite its potential benefits, several challenges remain to be addressed, including the correct assembly of the nanospheres on a

large-scale, the recovery of the immobilized enzyme from high-volume cultures or the achievement of sufficiently high expression levels. Furthermore, the implementation of enzyme reutilization at industrial scale is expected to be complex and key factors such as the removal of PET residues and the efficient recovery of the nanospheres will require thorough consideration and optimization.

5. Conclusion

In this work we present a novel "in cellulo" self-immobilization method for PET-degrading enzymes with outstanding potential advantages over previously developed strategies at small-scale. In addition to the simple and cost-effective production of the immobilized enzyme, the great reusability and efficient degradation of untreated post-consumer PET place our technology as a promising tool for plastic biorecycling. Furthermore, the versatility of our system opens the door to tailoring the immobilized catalyst by the co-immobilization with other synergistic enzymes or the functionalization of the carrier with PET binding modules [27,28,61,62]. Scaling-up as well as economic and life cycle analysis of the process will be also assessed in future work. Thus, IC-Tagging emerges as a powerful platform to support the industrial translation of PET-degrading enzymes, contributing towards a circular plastic economy.

Environmental Implication

PET, widely used in the packaging industry, is one of the main sources of plastic waste due to its non-biodegradable nature, accumulating in landfills and natural environments. To address this issue, enzymatic PET recycling has emerged as a sustainable alternative. This study presents a novel method for the "in cellulo" self-immobilization of PET-degrading enzymes, improving their stability and reusability. The immobilized enzyme achieved almost complete degradation of untreated post-consumer plastic in successive cycles. Additionally, the production method is potentially more efficient and cost-effective, further contributing to the translation of enzymatic PET recycling into a large-scale industrial process

CRediT authorship contribution statement

Gemma Eibes: Writing – review & editing, Supervision, Project administration, Funding acquisition, Formal analysis, Conceptualization. **Jose Martinez-Costas:** Writing – review & editing, Supervision, Project administration, Funding acquisition, Formal analysis, Conceptualization. **Adrián López-Teijeiro:** Writing – review & editing, Writing – original draft, Investigation, Formal analysis, Conceptualization. **Natalia Barreiro-Piñeiro:** Writing – review & editing, Investigation, Formal analysis, Conceptualization.

Ethics statement

No animals or human subjects were used in the above research.

Funding

This work was supported by the Spanish Ministerio de Ciencia, Innovación y Universidades [Grants PID2022-139720OB-I00, CNS2023-144997 and TED2021-131322B-I00], the Xunta de Galicia [Grant ED431C 2021/29 and Centro de Investigación do Sistema universitario de Galicia accreditation 2023–2027, ED431G 2023/03] and the European Union [European Regional Development Fund – ERDF]. A.L.T is the recipient of a Spanish Ministerio de Universidades FPU-Ph.D. Contract [FPU22/03342]. G. E. belongs to the Galician Competitive Research Group [GRC ED431C 2021/37] and the Cross-disciplinary Research in Environmental Technologies [CRETUS Research Center, ED431G 2023/12].

Declaration of Competing Interest

A.L.T., N.B.P. and J.M.C. are inventors of several patents regarding the encapsulation technology described in this manuscript: 1) ES2364182 B2; US10059745 B2; EP2535348 B1 (J.M.C.): 2) ES2980877 B2 (N.B.P., A.L.T. and J.M.C.). The patent protection does not limit the sharing of methodological details. All experimental materials and methods are thoroughly described to enable independent replication for scientific purposes. The utilization, adaptation and commercial exploitation of the IC-Tagging methodology are restricted and subjected to a licensing agreement.

Acknowledgements

The authors thank Novapet company for kindly providing the PET beads used in the study, Massimo Lazzari for helping with the DSC analysis and PET grinding, and Rebeca Menaya for excellent technical support.

Appendix A. Supporting information

Supplementary data associated with this article can be found in the online version at doi:10.1016/j.jhazmat.2025.138789.

Data availability

Data will be made available on request.

References

[1] Geyer, R., Jambeck, J.R., Law, K.L., 2017. Production, use, and fate of all plastics ever made. Sci Adv 3, e1700782.
[2] Napper, I.E., Thompson, R.C., 2023. Plastics and the environment. Annu Rev Env Resour 48, 55–79.
[3] Nisticò, R., 2020. Polyethylene terephthalate (PET) in the packaging industry. Polym Test 90, 106707.
[4] Ellis, L.D., et al., 2021. Chemical and biological catalysis for plastics recycling and upcycling. Nat Catal 4, 539–556.
[5] Singh, N., Walker, T.R., 2024. Plastic recycling: a panacea or environmental pollution problem. Npj Mater Sustain 2, 17.
[6] Borrelle, S.B., et al., 2020. Predicted growth in plastic waste exceeds efforts to mitigate plastic pollution. Science 369, 1515–1518.
[7] Jambeck, J.R., et al., 2015. Marine pollution. Plastic waste inputs from land into the ocean. Science 347, 768–771.
[8] Wright, S.L., Kelly, F.J., 2017. Plastic and human health: a micro issue? Environ Sci Technol 51, 6634–6647.
[9] Maddela, N.R., Kakarla, D., Venkateswarlu, K., Megharaj, M., 2023. Additives of plastics: entry into the environment and potential risks to human and ecological health. J Environ Manag 348, 119364.
[10] Rai, P.K., Lee, J., Brown, R.J., Kim, K.H., 2021. Environmental fate, ecotoxicity biomarkers, and potential health effects of micro-and nano-scale plastic contamination. J Hazard Mater 403, 123910.
[11] Leslie, H.A., et al., 2022. Discovery and quantification of plastic particle pollution in human blood. Environ Int 163, 107199.
[12] Posnack, N.G., 2021. Plastics and cardiovascular disease. Nat Rev Cardiol 18, 69–70.
[13] Tournier, V., et al., 2023. Enzymes' power for plastics degradation. Chem Rev 123, 5612–5701.
[14] Müller, R.J., Schrader, H., Profe, J., Dresler, K., Deckwer, W.D., 2005. Enzymatic degradation of poly (ethylene terephthalate): rapid hydrolyse using a hydrolase from T. fusca. Macromol Rapid Comm 26, 1400–1405.
[15] Sulaiman, S., et al., 2012. Isolation of a novel cutinase homolog with polyethylene terephthalate-degrading activity from leaf-branch compost by using a metagenomic approach. Appl Environ Micro 78, 1556–1562.
[16] Yoshida, S., et al., 2016. A bacterium that degrades and assimilates poly (ethylene terephthalate). Science 351, 1196–1199.
[17] Qiu, J., et al., 2024. A comprehensive review on enzymatic biodegradation of polyethylene terephthalate. Environ Res 240, 117427.
[18] Tournier, V., et al., 2020. An engineered PET depolymerase to break down and recycle plastic bottles. Nature 580, 216–219.
[19] Lu, H., et al., 2022. Machine learning-aided engineering of hydrolases for PET depolymerization. Nature 604, 662–667.
[20] Pfaff, L., et al., 2022. Multiple substrate binding mode-guided engineering of a thermophilic PET hydrolase. ACS Catal 12, 9790–9800.
[21] Bell, E.L., et al., 2022. Directed evolution of an efficient and thermostable PET depolymerase. Nat Catal 5, 673–681.

[22] Shi, L., et al., 2023. Complete depolymerization of PET wastes by an evolved PET hydrolase from directed evolution. Angew Chem Int Ed 135, e202218390.
[23] Ding, Z., et al., 2023. Rational redesign of thermophilic PET hydrolase LCCICCG to enhance hydrolysis of high crystallinity polyethylene terephthalates. J Hazard Mater 453, 131386.
[24] Hong, H., et al., 2023. Discovery and rational engineering of PET hydrolase with both mesophilic and thermophilic PET hydrolase properties. Nat Commun 14, 4556.
[25] Cui, Y., et al., 2024. Computational redesign of a hydrolase for nearly complete PET depolymerization at industrially relevant high-solids loading. Nat Commun 15, 1417.
[26] Seo, H., et al., 2025. Landscape profiling of PET depolymerases using a natural sequence cluster framework. Science 387, eadp5637.
[27] Arnal, G., et al., 2023. Assessment of four engineered PET degrading enzymes considering large-scale industrial applications. ACS Catal 13, 13156–13166.
[28] Yao, J., Liu, Y., Gu, Z., Zhang, L., Guo, Z., 2024. Deconstructing PET: Advances in enzyme engineering for sustainable plastic degradation. Chem Eng J 497, 154183.
[29] Pellis, A., Vastano, M., Quartinello, F., Herrero Acero, E., Guebitz, G.M., 2017. His-tag immobilization of cutinase 1 from Thermobifida cellulosilytica for solvent-free synthesis of polyesters. Biotechnol J 12, 1700322.
[30] Nikolaivits, E., Makris, G., Topakas, E., 2017. Immobilization of a cutinase from Fusarium oxysporum and application in pineapple flavor synthesis. J Agr Food Chem 65, 3505–3511.
[31] Kumari, V., Kumar, S., Kaur, I., Bhalla, T.C., 2017. Graft copolymerization of acrylamide on chitosan-co-chitin and its application for immobilization of Aspergillus sp. RL2Ct cutinase. Bioorg Chem 70, 34–43.
[32] Su, A., Shirke, A., Baik, J., Zou, Y., Gross, R., 2018. Immobilized cutinases: Preparation, solvent tolerance and thermal stability. Enzym Microb Tech 116, 33–40.
[33] Bai, J., et al., 2025. Development of a self-assembled dual-enzyme co-display platform on the surface of the natural “chitosan beads” of yeast spores. Int J Biol Macromol 286, 138308.
[34] Schwaminger, S.P., et al., 2021. Immobilization of PETase enzymes on magnetic iron oxide nanoparticles for the decomposition of microplastic PET. Nanoscale Adv 3, 4395–4399.
[35] Jia, Y., et al., 2021. Nano-immobilization of PETase enzyme for enhanced polyethylene terephthalate biodegradation. Biochem Eng J 176, 108205.
[36] Chen, K., Dong, X., Sun, Y., 2022. Sequentially co-immobilized PET and MHET hydrolases via Spy chemistry in calcium phosphate nanocrystals present high-performance PET degradation. J Hazard Mater 438, 129517.
[37] Li, Z., Chen, K., Yu, L., Shi, Q., Sun, Y., 2022. Fe3O4 nanoparticles-mediated solar-driven enzymatic PET degradation with PET hydrolase. Biochem Eng J 180, 108344.
[38] Zurier, H.S., Goddard, J.M., 2022. Directed immobilization of PETase on mesoporous silica enables sustained depolymerase activity in synthetic wastewater conditions. ACS Appl Bio Mater 5, 4981–4992.
[39] Zhu, B., Ye, Q., Seo, Y., Wei, N., 2022. Enzymatic degradation of polyethylene terephthalate plastics by bacterial Curli display PETase. Environ Sci Tech Let 9, 650–657.
[40] Lee, Y.L., et al., 2024. Cross-linked enzyme aggregates of polyethylene terephthalate hydrolyse (PETase) from Ideonella sakaiensis for the improvement of plastic degradation. Int J Biol Macromol 263, 130284.
[41] Zhang, W., et al., 2024. A customized self-assembled synergistic biocatalyst for plastic depolymerization. J Hazard Mater 477, 135380.
[42] Han, H., et al., 2024. Biochar immobilized hydrolase degrades PET microplastics and alleviates the disturbance of soil microbial function via modulating nitrogen and phosphorus cycles. J Hazard Mater 474, 134838.
[43] Zhang, S., et al., 2025. Scalable nanoplastic degradation in water with enzyme-functionalized porous hydrogels. J Hazard Mater 487, 137196.
[44] Fritzsche, S., et al., 2025. Recycling the recyclers: strategies for the immobilisation of a PET-degrading cutinase. Bioproc Biosyst Eng 1–15.
[45] Lu, D., et al., 2024. The enhancement of waste PET particles enzymatic degradation with a rotating packed bed reactor. J Clean Prod 434, 140088.
[46] Brandariz-Nunez, A., Menaya-Vargas, R., Benavente, J., Martinez-Costas, J., 2010. A versatile molecular tagging method for targeting proteins to avian reovirus muNS inclusions. Use in protein immobilization and purification. PLoS One 5, e13961.
[47] Brandariz-Nunez, A., Menaya-Vargas, R., Benavente, J., Martinez-Costas, J., 2010. IC-tagging and protein relocation to ARV muNS inclusions: a method to study protein-protein interactions in the cytoplasm or nucleus of living cells. PLoS One 5, e13785.
[48] Barreiro-Piñeiro, N., Lostalé-Seijo, I., Varela-Calviño, R., Benavente, J., Martínez-Costas, J.M., 2018. IC-Tagging methodology applied to the expression of viral glycoproteins and the difficult-to-express membrane-bound IGRP autoantigen. Sci Rep 8, 16286.
[49] Brandariz-Nunez, A., Otero-Romero, I., Benavente, J., Martinez-Costas, J.M., 2011. IC-tagged proteins are able to interact with each other and perform complex reactions when integrated into muNS-derived inclusions. J Biotechnol 155, 284–286.
[50] Pose-Boirazian, T., et al., 2021. Chemical and thermal stabilization of CotA laccase via a novel one-step expression and immobilization in muNS-Mi nanospheres. Sci Rep 11, 2802.
[51] Brandariz-Nunez, A., Menaya-Vargas, R., Benavente, J., Martinez-Costas, J., 2010. Avian reovirus μNS protein forms homo-oligomeric inclusions in a microtubule-independent fashion, which involves specific regions of its C-terminal domain. J Virol 84, 4289–4301.
[52] Pirillo, V., Pollegioni, L., Molla, G., 2021. Analytical methods for the investigation of enzyme-catalyzed degradation of polyethylene terephthalate. FEBS J 288, 4730–4745.
[53] Bååth, J.A., Borch, K., Westh, P., 2020. A suspension-based assay and comparative detection methods for characterization of polyethylene terephthalate hydrolases. Anal Biochem 607, 113873.
[54] Zhong-Johnson, E.Z.L., Voigt, C.A., Sinskey, A.J., 2021. An absorbance method for analysis of enzymatic degradation kinetics of poly (ethylene terephthalate) films. Sci Rep 11, 928.
[55] Thomsen, T.B., Schubert, S.W., Hunt, C.J., Westh, P., Meyer, A.S., 2023. A new continuous assay for quantitative assessment of enzymatic degradation of poly (ethylene terephthalate)(PET). Enzym Microb Tech 162, 110142.
[56] Erickson, E., et al., 2022. Comparative performance of PETase as a function of reaction conditions, substrate properties, and product accumulation. ChemSusChem 15, e202101932.
[57] Kawai, F., et al., 2022. Efficient depolymerization of polyethylene terephthalate (PET) and polyethylene furanoate by engineered PET hydrolase Cut190. Amb Express 12, 134.
[58] Avilan, L., et al., 2023. Concentration-dependent inhibition of mesophilic PETases on poly (ethylene terephthalate) can be eliminated by enzyme engineering. ChemSusChem 16, e202202277.
[59] Thomsen, T.B., Hunt, C.J., Meyer, A.S., 2022. Influence of substrate crystallinity and glass transition temperature on enzymatic degradation of polyethylene terephthalate (PET). New Biotechnol 69, 28–35.
[60] Maghraby, Y.R., El-Shabasy, R.M., Ibrahim, A.H., Azzazy, H.M.E.S., 2023. Enzyme immobilization technologies and industrial applications. ACS Omega 8, 5184–5196.
[61] Li, A., et al., 2023. Discovery and mechanism-guided engineering of BHET hydrolases for improved PET recycling and upcycling. Nat Commun 14, 4169.
[62] Miao, R., et al., 2024. Engineering dual-functional and thermophilic BMHETase for efficient degradation of polyethylene terephthalate. Bioresour Technol 414, 131556.